Available online at www.sciencedirect.com
ScienceDirect
Journal of Photochemistry and Photobiology A: Chemistry 183 (2006) 89–97
Journal of Photochemistry and Photobiology A:Chemistry
www.elsevier.com/locate/jphotochem

Experimental and theoretical study of 3-carboxy-5,6-benzocoumarin

Cristina Tablet, Andrei Jelea, Mihaela Hillebrand *

University of Bucharest, Faculty of Chemistry, Department of Physical Chemistry, Bd. Regina Elisabeta 4-12, Bucharest, Romania

Received 16 December 2005; received in revised form 22 February 2006; accepted 23 February 2006
Available online 3 April 2006

Abstract

The electronic absorption and emission spectra of 3-carboxy-5,6-benzocoumarin in organic solvents and in aqueous buffered media are reported and discussed. The experimental data allowed for the estimation of the ground state acidity constant, $pK_a = 4.6$. A significant larger fluorescence quantum yield was found for the undissociated form than for the carboxylate species. The solvent-dependent MO calculations, at both semiempirical and ab initio levels, outlined the role of the solvation processes in the ground state properties especially for the dissociated species. Considering the sequence of states calculated by the AM1 method at the geometry of S_0 and S_1, the wavelength of the absorption and emission bands were estimated. The agreement is good for the absorption maxima and only satisfactory for the fluorescence bands. The difference in the quantum fluorescence yields for the undissociated and dissociated species was explained in terms of a different probability of the ISC, $S_1 \rightarrow T_2$ process.

Keywords: Coumarin derivatives; Photophysical properties; Solvent-dependent MO calculations

1. Introduction

The coumarins represent a widely studied class of compounds with applications in several fields. Some derivatives in the coumarin class are fluorescent, their emission properties being influenced by several factors as the nature of substituents, position of substitution and solvents [1–7]. They are characterized by large Stokes shifts and a broad and featureless linear response in solution. Due to these properties the coumarin derivatives were utilized as laser dyes, ionophores, fluorescence markers and probe molecules for the examination of electron transfer processes and ultrafast solvation effects [8–20].

The improvement of the photophysical properties of coumarin derivatives directed towards a bathochromic shift of the fluorescence maximum, an increase of the Stokes shift without a significant loss in the fluorescence quantum yields is one of the actual preoccupation in many laboratories. One of the direction followed by Takadate and co-workers [21] was the effect of either linear (positions 6,7) or angular (positions 5,6 or 8,9) annellation. The authors found that maintaining the same substituents in position 3 of the coumarin ring, the linear annellated derivatives present larger Stokes shifts, but smaller quantum yields. Considering the angular annellation, the 5,6-benzocoumarin derivatives present better emission properties than the 8,9-derivatives.

Many of the coumarin analogues were found to be biologically active, used as anticoagulants. They bound to the serum proteins, this binding affecting their pharmacologic and pharmacokinetic properties [22–24].

Recent studies attest that some benzocoumarin derivatives present interaction with HIV reverse transcriptase and act as effective photocatalysts in the oxidative degradations under natural conditions. They were found as degradation products or metabolites of phenanthrene, i.e. 5,6-benzocoumarin was found as a metabolite in the degradation of phenanthrene by Sphingomonas sp. strain P2, in the extract of *Juncus acutus* rhizomes [25–30].

During the last years, our laboratory was involved in the characterization of the photophysical properties of some heteroaromatic compounds, in order to use them as fluorescent probes for proteins. Thus, in the class of phenoxathiin derivatives, we have shown that in spite of the low fluorescent quantum yield of the parent heterocycle, some derivatives have good enough emission properties to be used as fluorescent probes [31]. Moreover, the study of their inclusion complexes with cyclodextrin revealed an enhanced sensitivity to local polarity [32]. Starting from their

* Corresponding author. Tel.: +40 21 3143508/173.
E-mail address: mihh@gw-chimie.math.unibuc.ro (M. Hillebrand).

1010-6030/$ – see front matter © 2006 Elsevier B.V. All rights reserved.
doi:10.1016/j.jphotochem.2006.02.028

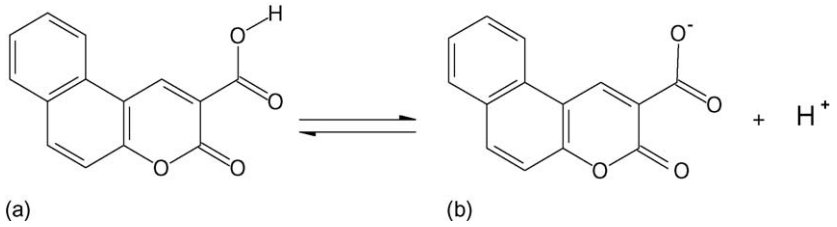

Fig. 1. Acid–base equilibrium for the 3-carboxy-5,6-benzocoumarinic acid.

photophysical properties, 2- and 3-carboxy-phenoxathiin [33] were chosen and their interaction with Bovine Serum Albumin (BSA) was studied by means fluorescence and NMR methods, revealing that at neutral pH they present a significant binding to the albumin [34]. Continuing on the same line, a new compound, a benzocoumarin derivative, the 3-carboxy-5,6-benzocumarin was considered.

According to literature data [21,33] we expect that this compound is suitable to be further used as protein probe. Due to the extension of the π system it is likely that its emission maximum will be well separated from the albumin emission. Moreover, owing to the possible acid (**a**)–base (**b**) equilibrium

$$\text{R-COOH} \rightarrow \text{R-COO}^- + \text{H}^+,$$

this compound has an enhanced solubility in aqueous media and would be suitable for studying protein interaction.

Prior to its utilization as a fluorescent probe, an experimental and theoretical characterization of the photophysical properties and the electronic structure of the excited states were necessary.

From the experimental point of view, the aim of this paper is the following: (i) to report a spectral study of the absorption and emission properties of this derivative in organic solvents and aqueous medium and (ii) to make an estimate of the dissociation constant of the acid–base equilibrium (Fig. 1).

As concerns the theoretical study, we focus on the ground (S_0) and excited singlet state (S_1) geometry, on the sequence of the excited singlet and triplet states at the optimized geometry of both S_0 and S_1 and the identification of the possible deactivation pathways.

Although there is now the possibility to obtain good estimate of the absorption maxima using the time dependent DFT method [35] and such calculations were previously made on other coumarin derivatives [36–38], we were more interested to obtain an overview on the prediction of both absorption and fluorescence spectra. Therefore, we choose the AM1 semiempirical method that allows for the optimization of the geometry of S_0 and S_1 states leading to the sequence of the energy levels at both geometries. As one of the species is a charged one, both in vacuo and solvent-dependent optimizations were made at the semiempirical level for S_0 and S_1 states and at the HF-ab initio level for S_0. The calculations using a solvation model are intended to emphasize the role of solvation in the theoretical modeling of the charged species. The problem is important, as most fluorofores used in ligand–protein interactions are charged species, whereas the molecular modeling of these interactions is usually performed neglecting the solvent effects.

2. Experimental part and MO calculations

The absorption and steady-state fluorescence spectra were recorded with a UNICAM-Heλios α spectrophotometer and an AMINCO-BOWMAN spectrofluorometer, respectively. The spectral measurements were made in spectroscopic grade solvents with different polarities: *n*-heptane (Fluka), cyclohexane (Merck), carbontetrachloride (Merck), dioxane (Aldrich), methylenechloride (Fluka), *n*-butanol (Aldrich), ethanol (Aldrich), methanol (Merck), dimethylsulphoxide (Fluka) and acetonitrile (Aldrich). They were checked for fluorescence and used without further purification.

The natural lifetime was calculated using the Strikler and Berg relation [39]:

$$\frac{1}{\tau_f^0} = 2.88 \times 10^{-9} \frac{g_1 n_f^3}{g_2 n_a} \frac{\int F(\nu)\,d\nu}{\int F(\nu)\nu^{-3}\,d\nu} \int \varepsilon(\nu)\nu^{-1}\,d\nu$$

in which the quantities have the following meanings: g_1, g_2—the multiplicities of the ground and excited states, n_a, n_f—the refractive indexes of the solvent at the wavelength of the absorption and fluorescence maxima; in our case we have considered $n_f = n_a$; $F(\nu)$ and $\varepsilon(\nu)$—the intensity at the emission maximum and the molar absorption coefficient.

In order to evaluate the integrals $\int(\varepsilon(\nu)/\nu)\,d\nu$ a deconvolution of the spectra was previously performed in cases of partially overlapping bands. The natural lifetime was estimated after the deconvolution of the absorption spectra and only the band on the longer wavelength range was considered.

The fluorescence quantum yields, Φ_f, were determined relatively to standard quinine sulphate in 1N sulphuric acid solution, $\Phi_{f0} = 0.55$ using solutions with the absorbance lower than 0.08. The estimated errors for the fluorescence measurements are about 10%. The Stokes shifts were calculated as the difference between the wavenumbers corresponding to the maxima of the absorption and emission bands.

Solvent-dependent semiempirical MO calculations for the ground and excited states were performed using the AM1 hamiltonian (AMSOL program) [40]. The optimizations were performed using the configuration interaction, C.I. = 2 and 3 and the Eigenvector Following and TRUSTE as optimizers. The solvation model was SM5.1 A [41–44]. The atomic charge densities were the Charge Model 1 (CM1) used in the solvent-dependent calculations. The geometry optimization of the excited states, considering a solvation model was more difficult to perform. The minima were rather flat and the gradients were only about 1–1.2 kcal/Å or radian. The potential energy surfaces (PES) in

respect with the torsion about the coumarin-substituent bond were built considering fixed values for the dihedral and allowing for a total relaxation of all the other coordinates. Hartree–Fock (HF) ab initio calculations for the ground state of both species **a** and **b** were carried out using the GAMESS program [45] and the 6-31G* basis set. The solvent effect was considered in the frame of the polarizable continuum model (PCM).

3. Results and discussions

3.1. Absorption and fluorescence spectra

3.1.1. Organic solvents

The absorption spectra of 3-carboxy-5,6-benzocoumarin in several solvents in which it was soluble enough are presented in Fig. 2, and the absorption maxima and absorptivities are listed in Table 1. In the range of 250–400 nm the spectra are characterized by two systems of bands.

The system of bands situated at larger wavelengths, which will be implicated in the emission process presents a more complicated aspect due to either a superposition of very closed electronic transitions or to a vibrational structure. In dioxane some vibrational peaks were observed. In protic solvents, the band exhibits only two maxima and is blue shifted, raising the problem of the n–π* or π–π* nature of the band. Considering both polarization experiments and theoretical calculations, the first band of coumarin was assigned to a π–π* transition, polarized along the long molecular axis and mainly localized on the 1,2-pyrone ring [46–48]. More recent studies attest that the photophysical properties of coumarin derivatives is determined by the relative position of the π–π* and n–π* states dependent on the substituents and the solvent polarity [49,50].

In our case, the presence of the COOH group could justify the implication of the non-bonding electrons, so the first transition could be considered an n–π* one. However, the values of the extinction coefficients plead for a π–π* character. The blue shift in polar protic solvents was also observed for other carboxylic compounds like the 9-anthroic carboxylic acid, the 9-acridincarboxylic acid [51,52] and the 3-carboxyphenoxathiin [33] and was explained by hydrogen bond interactions. Considering these arguments, we ascribe the band situated at 360–400 nm to a π–π* transition.

The emission spectra are dependent on the solvent polarity. The photophysical properties are also included in Table 1. In

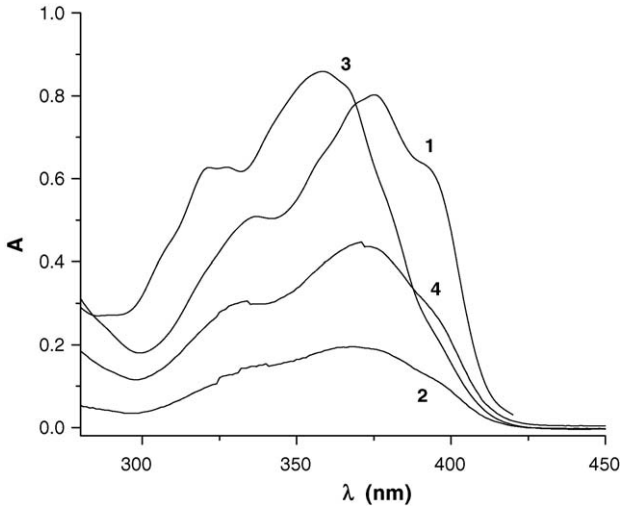

Fig. 2. Absorption spectra in solvents with different polarities: (1) dioxane; (2) *n*-butanol; (3) ethanol; (4) dimethylsulphoxide (DMSO).

protic media, ethanol and methanol, both a decrease in the fluorescence quantum yields and an increase in the Stokes shifts was noticed. Although for a compound containing an OH [53] or carboxylic group, it is difficult to separate the different effects which could influence the experimental behavior: the polarity of the solvents, the specific interactions due to the hydrogen bonds formation in protic solvents and the presence in different ratios of both the undissociated and dissociated forms, an attempt was made to estimate the increase in the dipole moment value upon excitation using the Lippert-Mataga equation [54,55]:

$$\nu_f = \nu_0 - \frac{2(\Delta\mu)^2}{hca^3}\left(\frac{\varepsilon - 1}{2\varepsilon + 1} - \frac{1}{2}\frac{n^2 - 1}{2n^2 + 1}\right)$$

$$F(\varepsilon, n) = \frac{\varepsilon - 1}{2\varepsilon + 1} - \frac{n^2 - 1}{2(2n^2 + 1)}$$

where ε and n are the dielectric constant and refractive index, a the Onsager cavity radius and $\Delta\mu$ is the increase of the dipole moment upon excitation.

The solvents used ranging from non-polar to polar are mentioned in Fig. 3. Considering a value of 3.92 Å for the Onsager cavity radius, estimated as 40% of the longest diam-

Table 1
Absorption and emission properties of 3-carboxy-5,6-benzocoumarin in organic solvents and aqueous medium

Solvent	λ_{abs} (nm)	ε (cm^{-1} M^{-1})	λ_f (nm)	FWHM (cm^{-1})	Stokes shift (cm^{-1})	τ_0 (ns)	Φ	τ_f^0(ns)
Dioxane	372	16560	428	4268.4	3517.2	25.1	0.53	13.3
n-Butanol	372	11000	440	3425.9	4154.5	33.3	0.27	9.0
Acetonitrile	376	16100	446	3198.1	4174.2	24.0	0.54	13.0
Ethanol	363	9600	429	3401.7	4238.2	34.4	0.07	2.4
Methanol	364	7900	431	3459.9	4270.7	24.0	0.10	2.4
pH 0.93 (aq)	376	[a]	460	3643.9	4659.5	[a]	0.41	[a]
pH 9.48 (aq)	360	3716	428	3980.0	4646.7	53.5	0.24	12.8

[a] Solubility too low to allow exact measurement.

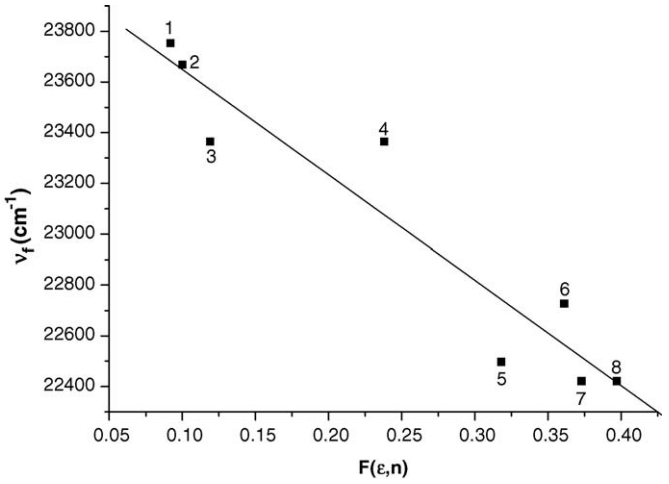

Fig. 3. Plot of fluorescence wavenumbers, ν_f, vs. the Lippert-Mataga solvent polarity function, $F(\varepsilon, n)$ ($r = 0.949$). The solvents are: (1) *n*-heptane; (2) cyclohexane; (3) carbontetrachloride; (4) dioxane; (5) methylenechloride; (6) *n*-butanol; (7) dimethylsulphoxide; (8) acetonitrile.

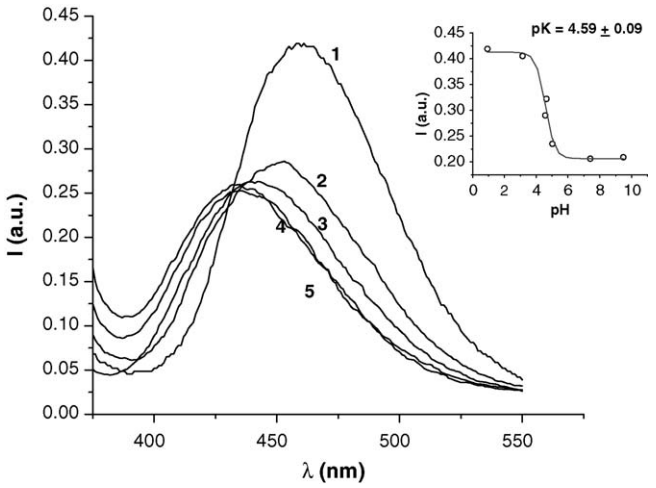

Fig. 4. Emission spectra in buffered solutions with different pH: (1) 0.93; (2) 3.85; (3) 5.02; (4) 7.40; (5) 9.48. *Inset*: The titration curve.

eter [56], the plot ν_f versus $F(\varepsilon, n)$ (Fig. 3) led to the value of $\Delta\mu = 5$ D.

3.1.2. Aqueous solution: pH dependence

The absorption and emission spectra in aqueous solution reflect a pH dependence rationalized in terms of the already mentioned acid–base equilibrium between the undissociated (**a**) and dissociated (**b**) forms.

The absorption maxima and the photophysical properties of both species in aqueous solutions at pH 0.93 and 9.48 are also included in Table 1. The low solubility of the compound at acid pH prevents an exact determination of the absorbance and, consequently, the natural lifetime.

The red shift of the maximum of **a** (376 nm, low pH) as compared to that of **b** (360 nm) reflects an enhanced substituent-cycle conjugation in the former case. According to the spectral data it is expected that **a** will adopt a planar conformation of the COOH group while the COO^- group could be stabilized by solvation in an orthogonal position in respect with the aromatic ring, decreasing the π conjugation.

The pH dependence of the fluorescence spectra is presented in Fig. 4. Increasing the pH, the spectrum shifts from 460 nm (low pH, species **a**) to 428 nm (pH > 7, species **b**). A fluorimetric titration allows for the estimation of the equilibrium constant of the dissociation process, $pK_a = 4.6$. The value obtained is in the range of the ground state dissociation constants reported for polycyclic aromatic and heteroaromatic carboxylic acids [57,58]. Considering literature data a larger value would be expected for the excited state.

A comparison of the emission intensities of both forms points out a value of 0.41 for the quantum yield of **a** and a lower value, 0.24 for **b**. This behavior is different from what was obtained for 3-carboxy-phenoxathiin [33] and shows different relative contributions of the radiative and non-radiative deactivation processes.

3.2. MO calculations

3.2.1. Geometries of the ground (S_0) and excited singlet (S_1) states

The correlation of the photophysical properties of the heteroaromatic carboxylic acids with the position of the carboxy or carboxylate group in respect with the aromatic fragment was extensively discussed [59–66]. Different positions of the COOH group in respect with the planar aromatic or heteroaromatic moieties are reported [51,52,57–66]. For example, the COOH group in positions 4 and 5 of indole is coplanar with the ring, whereas the same group in positions 2 and 3 is twisted in respect with the indole moiety [59–63]. Similar situations were encountered in anthracene and naphthalene carboxylic acids substituted at various positions [58]. The results are different from those predicted for 9-anthroic and 9-acridincarboxylic acids for which the interaction with the *peri* hydrogens prevents a coplanar position of the substituent even in the ground state [52]. The same effect was discussed by Manoharan and Dogra [64,65] for the structural and spectral features of some fluorencarboxylic acids.

In the class of carboxylic coumarin derivatives, the study of Coumarin 343 using the DFT method starts with five possible conformers, the last two corresponding to zwiterionic structures [36]. The authors found that the most stable conformer is that in which the OH group is directed towards the C=O of the coumarin ring allowing for a possible hydrogen bond.

In order to get information on the geometry of both **a** and **b** species, the ground and excited potential energy surfaces (PES) in respect with the torsion about the coumarin-substituent bond (τ_1) were calculated in different solvents using the AM1 method. Two values, 0° and 180°, were considered for the torsion describing the position of the carboxylic hydrogen (τ_2). The definition of the two dihedrals and the results for in vacuo and water calculations are plotted in Figs. 5 and 6.

The minimum energy conformers of the undissociated form **a** in the S_0 state (Fig. 5) were labeled as **I–IV**. It was found that in vacuo, all but **IV** adopt a planar conformation. Conformers **I** and **II** have practically the same energy. In water (Fig. 5) or

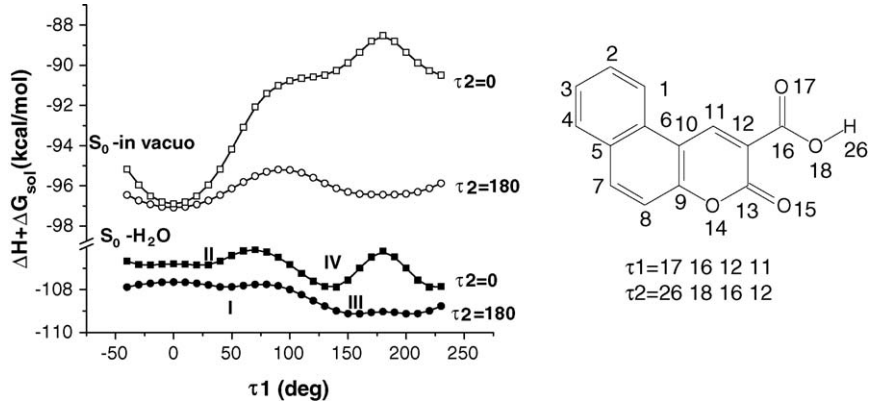

Fig. 5. In vacuo and water calculated sections through the potential energy surfaces of the undissociated species **a** along the torsion τ_1 describing the position of the COOH group relative to the benzocoumarin moiety.

Table 2
Semiempirical calculated values for the dihedral τ_1 (°), heat of formation and free energy of solvation, $\Delta H + \Delta G_{sol}$ (kcal/mol), dipole moments, μ (D), ring-substituent bond orders, p, for conformers **I** and **III** ($\tau_2 = 180°$) of species **a** and **b** in the ground state

	a				**b**	
	I	**I**	**III**	**III**		
	In vacuo	Water	In vacuo	Water	Water	Water
τ_1	0.8	4.7	176.9	155.1	179.2	90.1
$\Delta H + \Delta G_{sol}$	−97.09	−107.65	−96.44	−109.15	−194.15	−196.26
ΔG_{sol}	–	−10.57	–	−12.70	−71.61	−73.27
μ	5.85	9.73	7.66	13.37	–	–
$p_{ring\text{-}COOH}$	0.962	0.971	0.960	0.963	0.894	0.872

polar non-protic solvents (ACN—data not shown) the minima are shifted towards 40° and 160°, the conformer in which the C=O bond of COOH is directed towards the coumarin C=O (**III**) being favored. **IV** retains its non-planar structure but the barrier to rotation is strongly diminished to about 1–2 kcal/mol, so that we can consider a free rotation. Some theoretical data for **a** (in vacuo and water) and **b** (water) obtained after a fully optimization of the minimum energy points are listed in Table 2.

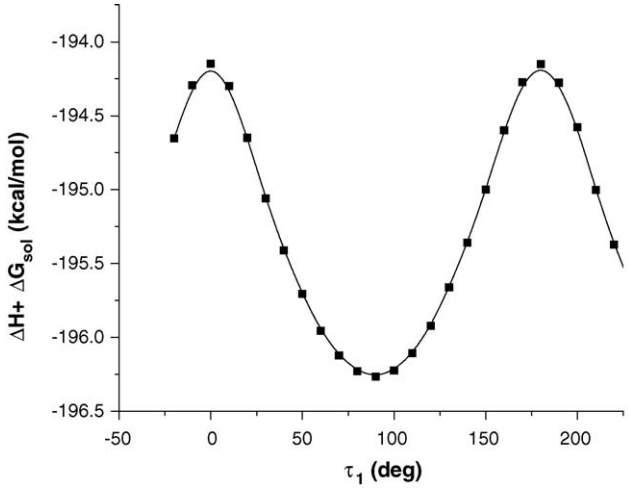

Fig. 6. Water calculated section through the potential energy surface of the dissociated species **b** along the torsion τ_1 describing the position of the COO^- group relative to the benzocoumarin moiety.

In the excited S_1 state, at both C.I. = 2 and 3, species **a** maintains its quasi-planar conformation but the barriers to rotation are somewhat higher, around 3–4 kcal/mol.

In the case of the dissociated species **b**, the minimum energy conformation in S_0 is the orthogonal one (Fig. 6). In the S_1 state, the theoretical results show no significant dependence of $\Delta H + \Delta G_{sol}$ on the torsion τ_1; the differences between conformers are lower than 0.1 kcal/mol, such that any conformation is possible.

As compared to the AM1 results, at the ab initio level, for both in vacuo and water calculations, a different order of stability of the four conformers was found. In this case, instead of **III** (AM1), conformer **II** was proved to be the most stable, in agreement with the results obtained by Cave and Castner for Coumarin 343. Therefore, in Table 3 the relative energies are calculated in respect with this conformer. It can be seen that the solvent determines a decrease in the energetic differences between the conformers, the effect being larger for the non-planar conformer **IV**, for which the solvation effects are more important. An estimation of the barrier to rotation at the ab ini-

Table 3
Ab initio, in vacuo and water calculated relative energies (E_{rel}, kcal/mol) of the conformers of **a**

	I	**II**	**III**	**IV**
E_{rel} (in vacuo)	3.75	0.00	5.60	14.45
E_{rel} (water)	3.01	0.00	2.04	8.65

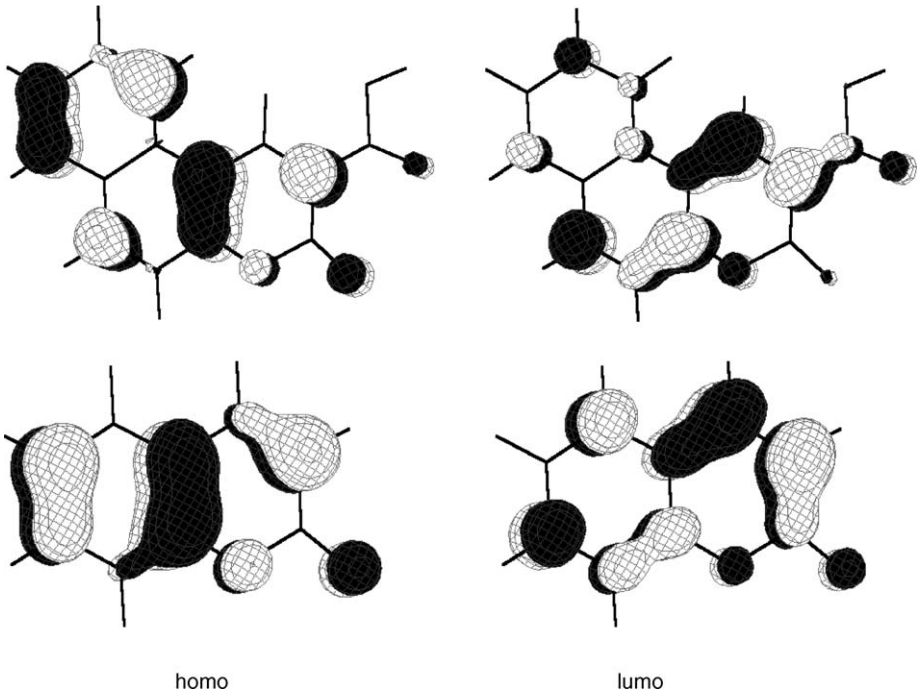

Fig. 7. Frontier molecular orbitals for the species **a** and unsubstituted coumarin.

tio level assuming that the energy for $\tau_1 = 90°$ represents the highest point on the potential energy surface for the conformational transition, leads to a value of about 5 kcal/mol. Therefore, in spite of the differences between the two approaches we can consider that all the conformers are thermally possible, with a lower probability for **IV**.

3.2.2. *Nature of the first excited state*

We have seen that the experimental data plead for a π–π^* character of the first electronic transition. The character of the first electronic transition, either n–π^* or π–π^*, a problem widely discussed for coumarin derivatives, is determined by the features of the frontier molecular orbitals. In the case of species **a**, the last two occupied molecular orbitals, *homo* and *homo*-1, hereafter labeled as A and B, respectively, as well as the first vacant orbital (*lumo*) are π orbitals localized on the three cycles without a significant contribution from the carboxy substituent, attesting the π–π^* nature of the S_1 state. The energies and the shape of these orbitals are only slightly influenced by the solvent (Fig. 7).

Apart a certain degree of localization on the 5,6 conjugated phenyl ring, these frontier molecular orbitals closely resemble the corresponding orbitals of coumarin, indicating that the first electronic transitions is dominated by the coumarin moiety of the molecule [67,68]. The same result, an insignificant contribution from the substituent, was also obtained for other substituted coumarin derivatives, 3-phenyl- and 3-thiophenyl-coumarin [69]. A different theoretical result was obtained for the dissociated species **b**. In the case of the in vacuo semiempirical calculations, the last three occupied molecular orbitals are totally localized on the substituent, implying a different nature of the first excited state. To distinguish them from the frontier orbitals of species **a**, these orbitals were hereafter labeled as C1, C2, C3 (carboxylates 1–3). The atomic coefficients are listed in Table 4.

The orbitals similar to *homo* and *homo*-1 of the neutral 3-carboxybenzocoumarin are located at lower energies. As the experimental data showed no major changes in the emission properties in going from the neutral to the dissociated species, it is difficult to assume a different nature of the implied singlet state. Therefore, the calculations were performed in different solvents and finally in water. The results are presented in Fig. 8. It can be observed that increasing the solvent polarity, the reversal of the orbital sequence is obtained, and in polar protic solvents an order similar with that of all the coumarin derivatives is obtained. As the dissociated species is present only in aqueous medium, only the water results are presented in Table 2. This points to the importance of performing solvent-dependent optimizations for charged molecular species.

At the ab initio level, the main features of the last occupied molecular orbitals of species **a** are similar to those obtained by semiempirical calculations.

The sequence of the frontier molecular orbitals for **b** is not correctly predicted even at the ab initio level. For the in vacuo calculations the order of the molecular orbitals is somewhat

Table 4
Expressions of C1, C2, C3, the three last occupied molecular orbitals of species **b**, totally localized on the atoms of the carboxy group, C, O1, O2 (in vacuo semiempirical calculations)

	ϕ
C1	$0.49\ px_{O1} + 0.54\ py_{O1} - 0.45\ px_{O2} + 0.49\ py_{O2}$
C2 (π)	$0.72\ pz_{O1} - 0.69\ pz_{O2}$
C3	$0.38\ px_{C} + 0.58\ px_{O1} + 0.62\ px_{O2}$

Table 5
Ab initio atomic population on the ring and carboxylate group in the four last occupied molecular orbitals of species **b**

	In vacuo				Water			
	homo-3, C3	*homo*-2, C2	*homo*-1, C1	*homo*, A	*homo*-3, C2	*homo*-2, C1	*homo*-1, B	*homo*, A
Ring	0.269	0.329	0.107	1.998	0.377	0.103	2.000	1.998
COO^-	1.731	1.671	1.893	0.002	1.623	1.897	0.000	0.002

improved as compared with the in vacuo AM1 calculation, i.e. *homo* has the expected shape similar with *homo* (A) in the neutral species, but *homo*-1 and *homo*-2 remain totally localized on the carboxylate group. Considering the solvent effect through the PCM model, the sequence of the orbitals is changed. The sum of the atomic populations on the benzocoumarin ring and the carboxylate for the four last occupied molecular orbitals of **b** for in vacuo and water optimization reflect well this fact. The results presented in Table 5 show that for the in vacuo calculations *homo*, A, is delocalized on the benzocoumarin ring whereas *homo*-1 preserves the features of C1. Introducing the solvent, the order of the orbitals becomes the expected one, A, B, C1, C2.

3.2.3. Charge distribution in the ground and excited states

The dipole moment values and the coumarin-substituent bond orders for conformers **I** and **III** are also listed in Table 2. As expected, the dipole moments are influenced by the position of the COOH group. Considering the bond order as a measure of the conjugation, the results reflect the decrease of substituent-coumarin conjugation in going from the neutral to the dissociated species.

In comparison with the ground state, an increase of the dipole moments was obtained in S_1, 9.25 D (conformer **I**) and 10.71 D (conformer **III**), reflecting the charge transfer character of the excited state. Considering the values in Table 2 for the ground state values, the predicted $\Delta\mu$ increase of about 4 D is in a satisfactory agreement with the experimental value previously determined.

Another observation concerning the excited state charge distribution consists in the significant change in the bond order values. The double bond character of the bond 3–4 in the coumarin cycle is strongly decreased, from 1.600 in S_0 to 1.300 in S_1 in agreement with the known photochemical behavior of coumarin derivatives. However, in comparison with the unsubstituted coumarin for which the corresponding values are 1.769 (S_0) and 1.356 (S_1) the differences are not so pronounced, reflecting a lower probability for a photodimerization process.

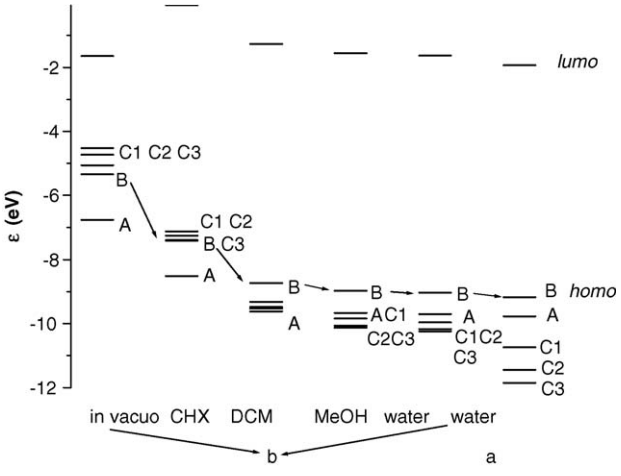

Fig. 8. Solvent dependence of the molecular orbitals of species **a** and **b**.

3.2.4. Absorption and emission spectra

According to the Frank-Condon principle, the absorption and emission maxima were estimated from the energy difference between S_1 and S_0, considering the sequence of levels calculated at the optimized geometry of S_0 and S_1, respectively. The calculations were performed at the C.I. = 3 level, i.e. considering the last two occupied molecular orbitals and the first vacant one. The diagrams of the energy levels and the estimated wavelengths for conformer **III** are presented in Fig. 9 and in Table 6, respectively. The fluorescence maxima for both species are predicted at 444 and 387 nm, respectively. The emission band is assigned to the *homo–lumo* transition with no contribution from the other excited configurations. The calculation of the absorption and emission maxima for the other conformers led to values in the same range, 338–346 nm for absorption and 437–450 nm for fluorescence, that is not unexpected as the frontier orbitals

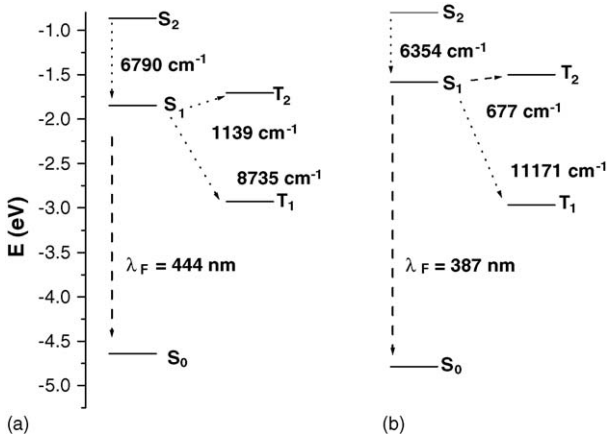

Fig. 9. Sequence of states for species **a** and **b** calculated in water at the optimized geometry of the first excited state S_1 (C.I. = 3).

Table 6
Experimental and calculated (C.I. = 3, water) absorption and emission wavelengths (λ, nm) for species **a** and **b**

	λ_a (exp)	λ_a (calc)	λ_f (exp)	λ_f (calc)
a	376	376	460	444
b	360	327	428	387

are practically localized on the coumarin ring with small contribution from the substituent.

The calculated wavelengths agree in a satisfactory way with the experimental data for species **a**, but are smaller for species **b**. However, the hypsochromic shift of the emission band in going from the undissociated to the dissociated species is correctly predicted.

Considering the possible non-radiative deactivation pathways it can be seen from Fig. 9 that for both neutral and dissociated forms, the S_1–T_1 gap is large enough to prevent the deactivation by intersystem crossing. However, the different values of the fluorescent quantum yields obtained for both species attest the probability of other non-radiative deactivation process, especially for **b**. The sequence of the excited states presented in Fig. 9 shows that the $|S_1–T_2|$ gap is lower for **b** as compared to **a**. Accordingly to literature data [70] an ISC process could be assumed if a triplet state is located above the singlet with at most 1000 cm^{-1}.

4. Conclusions

The experimental data show that the investigated compound, 3-carboxy-5,6-benzocoumarin acid can be used as a fluorescence probe but in organic solvents with medium polarity. In aqueous media the results are pH dependent and in neutral and basic pH, the dissociated form **b** is the predominant species; although its fluorescence quantum yield is lower than for the neutral form, it is high enough for being used as a fluorescent probe for proteins. The theoretical studies outlines the importance of introducing the solvation processes in the calculations especially for the charged species.

References

[1] R. Giri, S.S. Rathi, M.K. Machwe, Acta Phys. Hung. 70 (1991).
[2] J. Seixas de Melo, P.F. Fernandes, J. Mol. Struct. 565–566 (2001) 69–78.
[3] C. Vijila, A. Ramalingam, P.K. Palanisamy, V. Masilamani, Spectrochim. Acta Part A 57 (2001) 491–497.
[4] S. Kumar, R. Giri, S.C. Mishray, M.K. Machwe, Spectrochim. Acta Part A 51 (1995) 1459–1467.
[5] L. Taneja, A.K. Sharme, R.D. Singh, J. Lumin. 63 (1995) 203–214.
[6] A. Ramalingam, B.M. Sivaram, P.K. Palanisamy, V. Masilamani, Spectrochim. Acta Part A 56 (2000) 1205–1210.
[7] G. Jones II, W.R. Jackson, C. Choi, J. Phys. Chem. 89 (1985) 294–300.
[8] F. Gao, Dyes Pigments 52 (2002) 223–230.
[9] R.M. Christie, C.-H. Lui, Dyes Pigments 47 (2000) 79–89.
[10] V.K. Sharma, P.D. Sahare, A. Pandey, D. Mohan, Spectrochim. Acta Part A 59 (2003) 1035–1043.
[11] N.A. Nemkovich, W. Baumann, H. Reiss, Y.V. Zvierivich, J. Photochem. Photobiol. A: Chem. 109 (1997) 287–292.
[12] H. Shirota, H. Pal, K. Tominaga, K. Yoshihara, Chem. Phys. 236 (1998) 355–364.
[13] S. Nad, H. Pal, J. Photochem. Photobiol. A: Chem. 134 (2000) 9–15.
[14] S. Nad, H. Pal, J. Phys. Chem. A 104 (2000) 673–680.
[15] Y. Suzuki, N. Saito, H. Komatsu, D. Citterio, T. Kubota, Y. Kitamura, K. Oka, K. Suzuki, Anal. Sci. 17 (Suppl.) (2001) i1451–i1454.
[16] G. Jones II, J.A.C. Jimenez, J. Photochem. Photobiol. B: Biol. 65 (2001) 5–12.
[17] K. Setsukinai, Y. Urano, K. Kikuchi, T. Higuchi, T. Nagano, J. Chem. Soc., Perkin Trans. 2 (2000) 2453–2457.
[18] F. Cichos, R. Brown, U. Rempel, C. von Borczyskowski, J. Phys. Chem. 103 (1999) 2506–2512.
[19] S.K. Pal, D. Sukul, D. Mandal, S. Sen, K. Bhattacharyya, J. Phys. Chem. B 104 (2000) 2613–2616.
[20] M.L. Horng, J.A. Gardecki, A. Papazyan, M. Maroncelli, J. Phys. Chem. 99 (1995) 17311–17337.
[21] C. Murata, T. Masuda, Y. Kamochi, K. Todoroki, H. Yoshida, H. Nohta, M. Yamaguchi, A. Takadate, Chem. Pharm. Bull. 53 (2005) 750–758.
[22] J. Shobini, A.K. Mishra, K. Sandhya, N. Chandra, Spectrochim. Acta Part A 57 (2001) 1133–1147.
[23] W.W. Mantulin, P.-S. Song, J. Am. Chem. Soc. 95 (1973) 5122–5129.
[24] J. Llano, J. Raber, L.A. Eriksson, J. Photochem. Photobiol. A: Chem. 154 (2003) 235–243.
[25] C. Karapire, H. Kolancilar, U. Oyman, S. Icli, J. Photochem. Photobiol. A: Chem. 153 (2002) 173–184.
[26] M. DellaGreca, A. Fiorentino, M. Isidori, L. Previtera, F. Temussi, A. Zarelli, Tetrahedron 59 (2003) 4821–4825.
[27] M. Bilban, A. Billich, M. Auer, P. Nussbaumer, Bioorg. Med. Chem. Lett. 10 (2000) 967–969.
[28] I. Petitpas, A.A. Bhattacharya, S. Twine, M. East, S. Curryi, J. Biol. Chem. 276 (2001) 22804–22809.
[29] N. Mazzei, E. Sottofatori, M. Ibrahim, A. Balbi, Nucleosides Nucleotides 17 (1998) 1885–1889.
[30] O. Pinyakong, H. Habe, N. Supaka, P. Pinpanichkarn, K. Juntongjin, T. Yoshida, K. Furihata, H. Nojiri, H. Yamane, T. Omori, FEMS Microbiol. Lett. 191 (2000) 115–121.
[31] S. Ionescu, D. Gavriliu, O. Maior, M. Hillebrand, J. Photochem. Photobiol. A: Chem. 124 (1999) 67–73.
[32] M. Oana, A. Tintaru, D. Gavriliu, O. Maior, M. Hillebrand, J. Phys. Chem. B 106 (2002) 257–263.
[33] A. Tintaru, M. Oana, D. Gavriliu, M. Hillebrand, Rev. Roum. Chim. 49 (2004) 317–326.
[34] L. Birla, A.M. Cristian, D. Gavriliu, O. Maior, M. Hillebrand, Rev. Roum. Chim. 47 (2002) 769–775.
[35] D. Guillamont, S. Nakamura, Dyes Pigments 46 (2000) 85–92.
[36] R.J. Cave, E.W. Castner Jr., J. Phys. Chem. A 106 (2002) 12117–12123.
[37] R.J. Cave, K. Burke, E.W. Castner Jr., J. Phys. Chem. A 106 (2002) 9294–9305.
[38] J. Preat, D. Jacquemin, E.A. Perpete, Chem. Phys. Lett. 415 (2005) 20–24.
[39] J. Strikler, R. Berg, J. Chem. Phys. 37 (1962) 814–821.
[40] G.D. Hawkins, G.D. Giesen, G.C. Lynch, C.C. Chambers, I. Rossi, J.W. Storer, J. Li, T. Zhu, D. Rinaldi, D.A. Liotard, C.J. Cramer, D.G. Truhlar, AMSOL-6.5.3, University of Minnesota, Minneapolis, 1997.
[41] GAMESS,. M. Schmidt, K.K. Baldridge, J.A. Boatz, S.T. Elbert, M.S. Gordon, J.J. Jensen, S. Koseki, N. Matsunaga, K.A. Nguyen, S. Su, T.L. Windus, M. Dupuis, J.A. Montgomery, J. Comput. Chem. 14 (1993) 1347–1359.
[42] C.J. Cramer, D.G. Truhlar, J. Am. Chem. Soc. 113 (1991) 8305–8311.
[43] J.W. Storer, D.J. Giesen, C.J. Cramer, D.G. Truhlar, J. Comp. Aided Mol. Des. 9 (1995) 87–110.
[44] C.C. Chambers, C.J. Cramer, D.G. Truhlar, J. Phys. Chem. 100 (1996) 16385.
[45] D.J. Griesen, C.J. Cramer, D.G. Truhlar, Theor. Chem. Acta 98 (1997) 85.
[46] P.-S. Song, W.H. Gordon III, J. Phys. Chem. 74 (1970) 4234–4240.
[47] T.A. Moore, M.L. Harter, P.-S. Song, J. Mol. Spectrosc. 40 (1971) 144–157.
[48] R.H. Abu-Eittah, B.A.H. El-Tawil, Can. J. Chem. 63 (1985) 1173–1179.
[49] J. Seixas de Melo, R.S. Becker, F. Elisei, A.L. Macanita, J. Chem. Phys. 107 (1997) 6062–6069.
[50] J. Seixas de Melo, R.S. Becker, A.L. Macanita, J. Phys. Chem. 98 (1994) 6054.
[51] R.A. Agbaria, M.T. Butterfield, I.M. Warner, J. Phys. Chem. 100 (1996) 17133–17137.
[52] J. Dey, J.L. Haynes III, I.M. Warner, A.K. Chandra, J. Phys. Chem. A 101 (1997) 2271–2278.

[53] A. Morimoto, T. Yatsuhashi, T. Shimada, L. Biczok, D.A. Tryk, H. Inoue, J. Phys. Chem. A 105 (2001) 10488–10494.
[54] N. Mataga, Y. Kaifu, M. Koizumi, Bull. Chem. Soc. Jpn. 28 (1955) 690.
[55] E. Lippert, Z. Naturforsch. 10a (1955) 541.
[56] S.I. van Dijk, P.G. Wiering, C.P. Groen, A.M. Brouwer, J. Verhoeven, J. Chem. Soc., Faraday Trans. 91 (1995) 2107–2114.
[57] S.G. Schulman, I. Pace, J. Phys. Chem. 76 (1972) 1996–1999.
[58] P.J. Kovi, S.G. Schulman, Anal. Chim. Acta 63 (1973) 39–52.
[59] M. Krishnamurthy, A.K. Mishra, S.K. Dogra, Photochem. Photobiol. 45 (1987) 359.
[60] M. Krishnamurthy, H.K. Sinha, S.K. Dogra, J. Lumin. 35 (1986) 343–348.
[61] J.J. Aaron, A. Tine, M.E. Wojciechovska, C. Parkanyi, J. Lumin. 33 (1985) 33.
[62] P.S. Song, W.E. Kurtin, J. Am. Chem. Soc. 91 (1962) 4982.
[63] R.M. Linares, A. Gonzalez, J.H. Ayata, A.M. Afonso, V. Gonzalez, Spectrochim. Acta A 513 (1995) 1691–1701.
[64] R. Manoharan, S.K. Dogra, Spectrochim. Acta A 43 (1987) 91–100.
[65] R. Manoharan, S.K. Dogra, J. Photochem. Photobiol. A: Chem. 43 (1988) 119–137.
[66] M.K. Nayak, S.K. Dogra, J. Photochem. Photobiol. A: Chem. 161 (2004) 169–183.
[67] P.K. McCarthy, G.J. Blanchard, J. Phys. Chem. 97 (1993) 12205–12209.
[68] A. Muhlpfordt, R. Schanz, N.P. Ernsting, V. Farztdinov, S. Grimme, Phys. Chem. Chem. Phys. 1 (1999) 3209–3218.
[69] S. Ionescu, M. Hillebrand, Chem. Phys. 293 (2003) 53–64.
[70] N.I. Nijegorodov, V. Ramachandran, D.P. Winkoun, Spectrochim. Acta A 53 (1997) 1813–1824.